1. Kinga TOKARSKA[1], 2. Marek CIURYS[1]

Wroclaw University of Science and Technology
ORCID: 2. 0000-0002-7811-2198

doi:10.15199/48.2024.07.40

Computational analysis of a BLDC motor for a hoverboard

Abstract. *The article presents a computational analysis of the influence of selected dimensions of the magnetic circuit of a brushless DC motor intended to drive an electric board on the value of the cogging torque and the electromagnetic torque. Based on computations made using the developed field-circuit model, the target dimensions of the magnetic circuit were selected, and the waveforms of electrical and mechanical quantities as well as the electromechanical characteristics of the motor were determined. The results of the computation confirmed the assumed motor parameters.*

Streszczenie. *W artykule przedstawiono analizę obliczeniową wpływu wybranych wymiarów obwodu magnetycznego silnika bezszczotkowego prądu stałego przeznaczonego do napędu deski elektrycznej na wartość momentu zaczepowego oraz na moment elektromagnetyczny. Na podstawie obliczeń wykonanych za pomocą opracowanego modelu polowo-obwodowego dobrano docelowe wymiary obwodu magnetycznego oraz wyznaczono przebiegi wielkości elektrycznych i mechanicznych oraz charakterystyki elektromechaniczne silnika. Wyniki obliczeń potwierdziły zakładane parametry silnika. (**Analiza obliczeniowa silnika do napędu deski elektrycznej**).*

Keywords: BLDCM, brushless DC motor, permanent magnets, hoverboard.
Słowa kluczowe: BLDCM, silnik bezszczotkowy prądu stałego, magnesy trwałe, deska elektryczna.

Introduction

In recent years, there has been an increase in the popularity of electric vehicles. It is the result of research and development work carried out in the field of batteries and modern cooling methods of electric motors [1÷5]. This is also influenced by the effort to replace combustion cars with electric vehicles, which is motivated by reducing: exhaust emissions, greenhouse gases, and the use of fossil fuels. According to [6], in 2017 in the European Union, transport was responsible for 27% of carbon dioxide emissions from fuel combustion, of which up to 72% concern road transport. As a result, more and more countries are introducing regulations to protect the environment. These activities also aim to promote the use of electric vehicles or manifest themselves in the introduction of restrictions on the access to city centres for vehicles powered by combustion engines [7].

In 2010, the intergovernmental forum Electric Vehicles Initiative (EVI) was established as part of the Clean Energy Ministerial (CEM). The general goal of the activity is to accelerate the electrification of transport on a global scale. From 2020, one of the EVI member states is Poland [8,9].

Many leading automotive manufacturers are withdrawing internal combustion engines from further research to develop new electric vehicle designs. The awareness of environmental protection by society is also growing. More and more residents of urban agglomerations are choosing public transport. However, getting around cities, especially during the so-called rush hours, is becoming more and more inconvenient. An alternative solution is to have a small electric vehicle, which allows us to travel to school or work without traffic jams.

Despite the visible development of the electric vehicle market, the decreasing prices and the increasing range of electric cars, for many their price is still too high. At the same time, we can observe an increase in the popularity of smaller vehicles such as scooters or electric boards, which are a response to the requirements of potential users: fast and comfortable transport while maintaining the compactness of the vehicle.

These types of vehicles use low-power motors characterised by low weight and high power density. For this reason, brushless direct current (BLDC) motors are most often used.

The use of electrical boards is becoming more and more widespread. The value of the hoverboard market in 2020 is estimated at $1.4 billion. However, the expected increase in value in 2027 is $0.5 billion [10]. Hoverboards can improve travel comfort but also relieve the burden of people pushing, for example, baby strollers, shopping carts, or wheelchairs for disabled people [11]. For the reasons mentioned above, the paper focused on the BLDC motor intended for hoverboard drive.

The aim of the work was to design a BLDC motor intended to drive a hoverboard, develop its field-circuit model, and perform a computational analysis of the influence of permanent magnets angle and stator slots shapes on the cogging torque and electromagnetic torque in order to select the final design solution of the motor, as well as to determine the waveforms of electrical and mechanical quantities and electromechanical characteristics of the motor to confirm its assumed parameters.

Brushless DC motor design

A low-speed brushless DC motor with an external rotor built into the vehicle wheel was initially designed. The magnetic circuit of the pre-designed motor is shown in Figure 1. It is a motor with the following assumed parameters: power P = 350 W, speed n = 400 rpm, and voltage U = 36 V [12]. There are three kidney-shaped holes in the stator magnetic circuit. This shape and its arrangement do not interfere with the flow of the magnetic flux but reduce the weight of the motor.

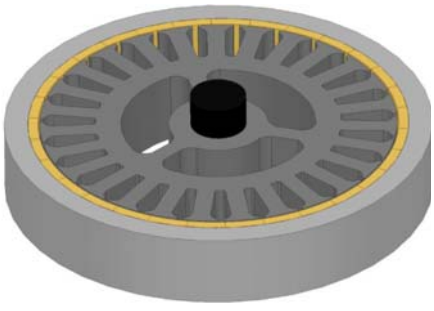

Fig.1. Magnetic circuit of the motor

It is a multipole motor with a non-integer ratio of the number of stator slots to the number of rotor poles. The number of magnets is 30 and the number of slots is 27. This design reduces the value of the cogging torque. The material of PMs is N33H with residual induction Br = 1,17 T and coercivity Hc = 883 kA/m. To ensure a high value of magnetic flux density and a trapezoidal field distribution in the air gap, radial magnetisation of magnets was used. The

electrical sheet M400-50A was used for the laminated stator core. Three-phase, single-layer, star-connected, concentrated, fractional stator winding was applied. To shorten the length of the end-connections and their overhang, a winding was used in which coils of the same phase are wound on adjacent stator teeth, but in the opposite direction. This type of winding reduces: copper weight, motor length, and power losses in the winding, and consequently, reduces motor heating. The winding diagram is shown in Figure 2.

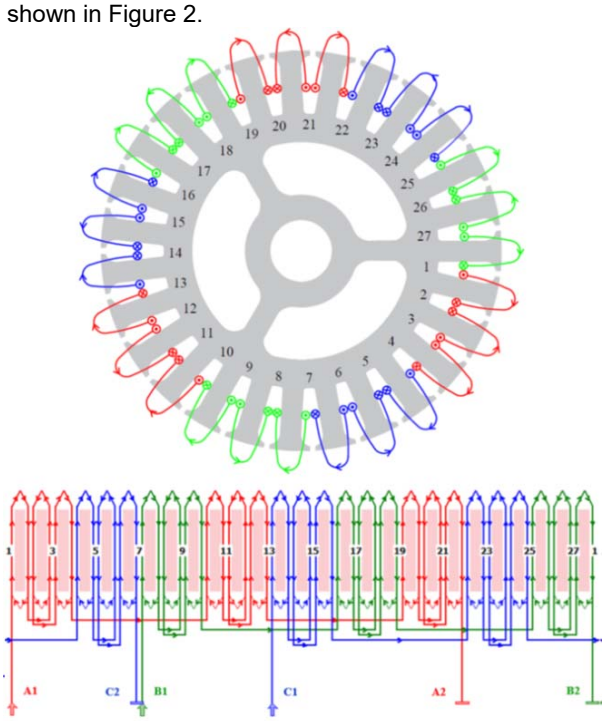

Fig.2. Winding diagram of the modelled motor (A1,A2,B1,B2,C1,C2 – beginnings and ends of the winding phases)

Brushless DC motor model

To analyse the influence of the dimensions of the motor's magnetic circuit on the value of the cogging and electromagnetic torque, select the target design, and determine the waveforms of electrical and mechanical quantities as well as electromechanical characteristics, a field-circuit model of the motor was developed. The model was developed using ANSYS software. The complete geometry of the motor was taken into account.

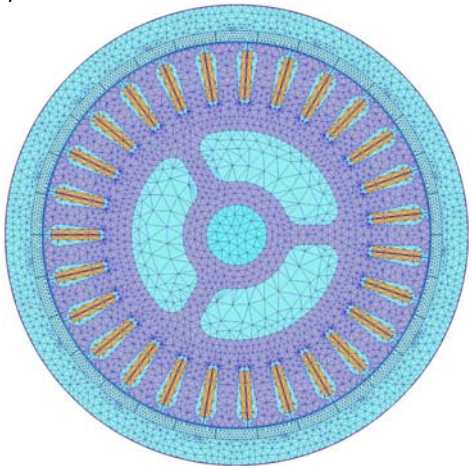

Fig.3. Brushless DC motor model with discretization mesh

A view of the developed field part of the model along with the discretization mesh is shown in Figure 3. The circuit part of the model is shown in Figure 4.

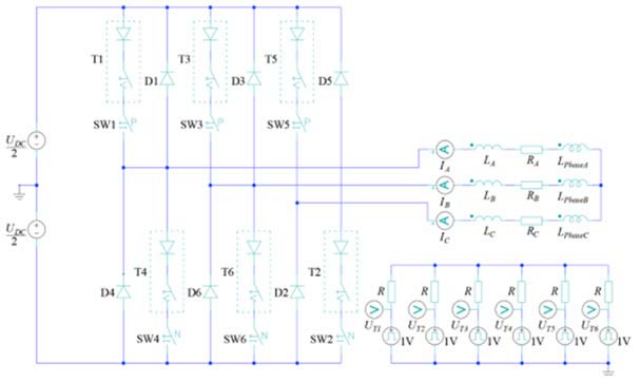

Fig.4. Diagram of the circuit part of the BLDC motor model

The field-circuit model of the motor takes into account, among others, the following factors:
− geometrical dimensions of the magnetic circuit,
− magnetisation characteristics of the rotor yoke and stator sheet materials,
− demagnetisation characteristics of permanent magnets,
− conductivity of the materials of the rotor yoke, stator sheets, and permanent magnets,
− eddy currents and hysteresis power losses in the stator and in the rotor,
− winding power losses,
− resistance and inductance of the winding (including the resistance and inductance of the winding end-connections),
− commutation of the winding phases,
− possibility of taking into account the limitation of instantaneous values of phase currents.

The field-circuit model is described in detail in [13].

Electromagnetic computations result

The motor to drive an electric board should provide the highest possible electromagnetic torque density [12]. For this reason, a computational analysis was carried out using the developed field-circuit model to select the dimensions of the magnetic circuit, ensuring the maximum average torque value. The motor design presented in Figure 3 was assumed as the base model.

An analysis of the influence of the permanent magnets angle and the shape of the stator slots on the analysed quantities was carried out. The analysis was carried out for the current excitation corresponding to the rated motor load torque. The analysis was performed for six different slots shapes (Fig. 5).

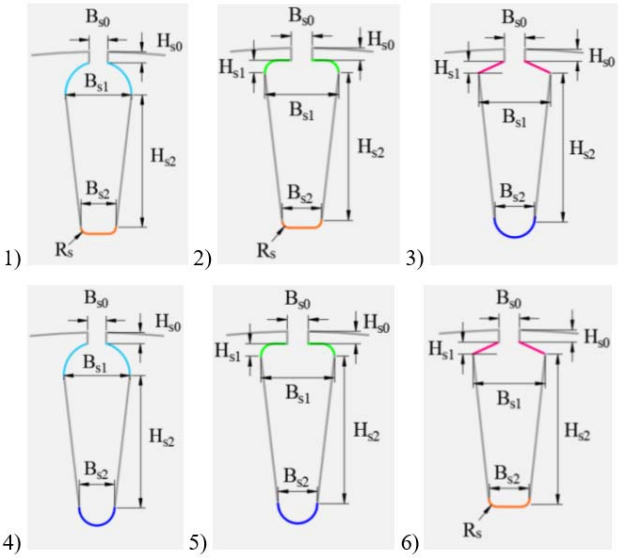

Fig.5. Analysed shapes of the stator slots

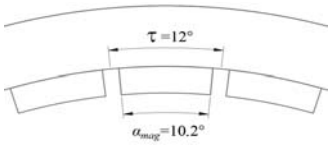

Fig.6. Sample value of the analysed magnet angle α_{mag}

Computations were made for angles α_{mag} (Fig.6) ranging from 6 to 12 degrees, which corresponds to the range from half of the pole pitch τ to the full pole pitch.

Figures 7 and 8 show the determined dependencies of the electromagnetic torque and the cogging torque on the rotor position angle at different values of the magnets angle. These results concern the no. 3 shape of slots (Fig.5). Analogous relationships were determined for the remaining analysed slots. Computations were made in the range of rotor positions between the winding phase switches.

Figure 9 shows the dependence of the average value of the electromagnetic torque on the angle of the magnets for the analysed slots. The dependences of the average value of the electromagnetic torque on the magnet angle are similar for all analysed shapes of the stator slots, however, the highest average value of the electromagnetic torque is obtained for the slot no. 6. The least favourable shape of the stator slot among those analysed is the shape no. 4.

Due to the assumed criterion of obtaining a high value of electromagnetic torque at a relatively small angle of the magnets, it was decided to choose the shape of slot no. 6 and the magnets angle of 10.2 degrees. There is no point in increasing the magnet angle above the selected value. The maximum increase in the average value of the electromagnetic torque that can be obtained is 1.61% when the magnet angle is increased by 17.65%.

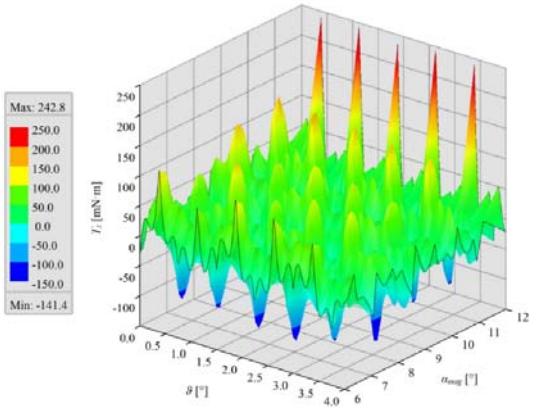

Fig.7. Dependence of the cogging torque on the angle of rotor position ϑ at different values of the magnets angle α_{mag} for the slot no. 3

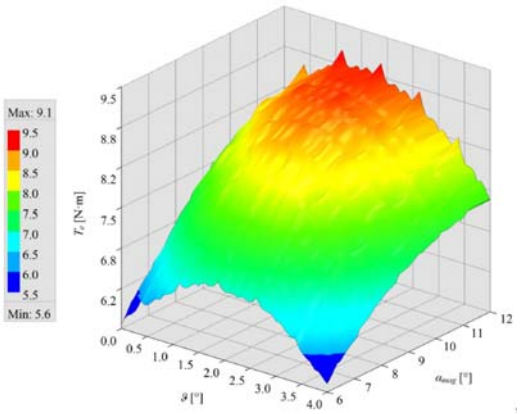

Fig.8. Dependence of the electromagnetic torque on the angle of rotor position ϑ at different values of the magnets angle α_{mag} for the slot no. 3

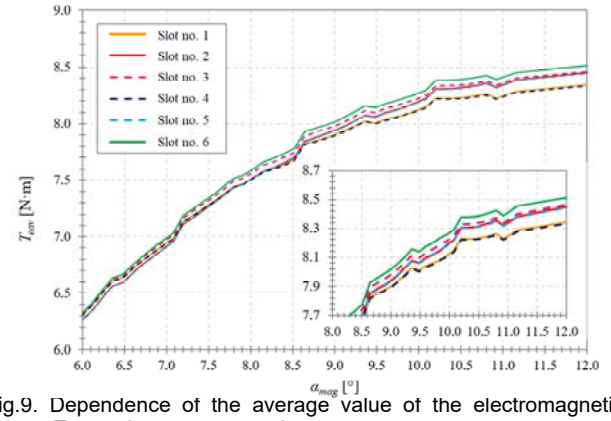

Fig.9. Dependence of the average value of the electromagnetic torque T_{eav} on the magnets angle α_{mag}

Waveforms of electrical and mechanical quantities of the motor

The waveforms of electrical and mechanical quantities were determined for the final motor design. The waveforms were determined for different values of the load torque. The current waveforms at the converter input and one of the motor phase currents are shown in Figures 10 and 11, respectively.

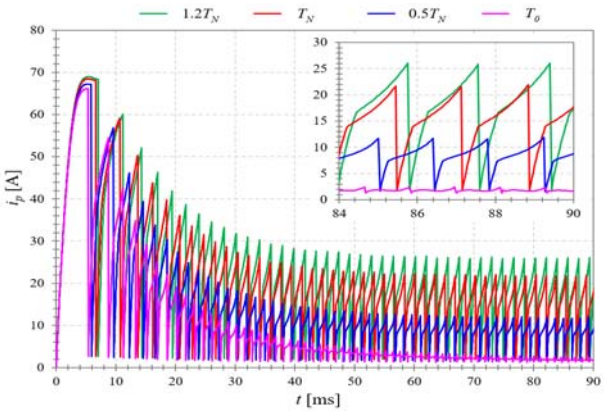

Fig.10. Current waveforms at the converter input at different values of the load torque

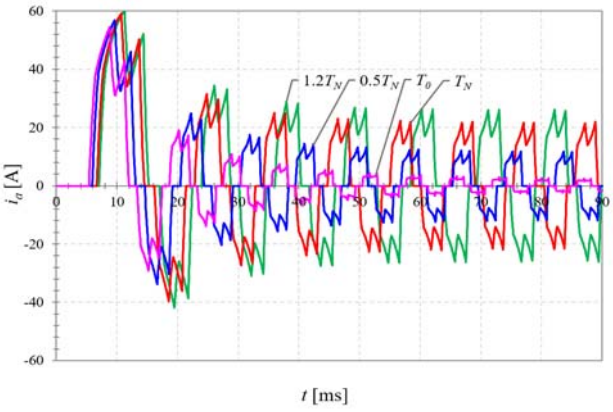

Fig.11. Waveforms of i_a phase currents at different values of the load torque.

The converter input current periodically increases and decreases as a result of cyclic switching of the power supply to the stator winding phases. This switching takes place every 60 electrical degrees based on information from the rotor position sensors. This corresponds to four mechanical degrees. In order to illustrate the influence of the load torque value on phase currents, Figure 11 shows the waveforms of the currents of one phase (phase *a*). The computed shapes are typical for brushless DC motors. The phase currents *a*, *b* and *c* are shifted by 120 electrical

degrees. Figures 12 and 13 show the waveforms of the electromagnetic torque and speed of the motor for four different load torque values.

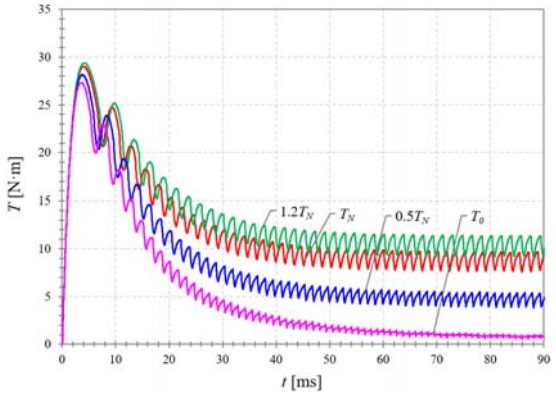

Fig.12. Waveforms of the motor electromagnetic torque at different values of the load torque

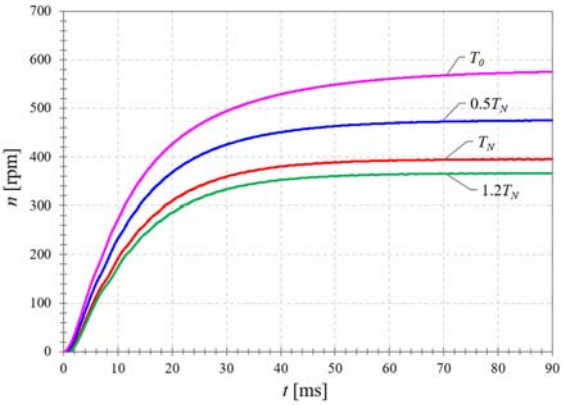

Fig.13. Waveforms of the motor speed at different values of the load torque

The performed computational analysis showed that a higher load torque value results in a lower rotational speed and also results in a larger amplitude of the motor torque pulsations. However, the effect on rotational speed pulsations is unnoticeable. It is damped by the motor moment of inertia. The lower speed results in a change in the switching frequency of the power converter transistors, which affects the frequency of voltages and phase currents of the motor, but also the frequency of torque pulsations.

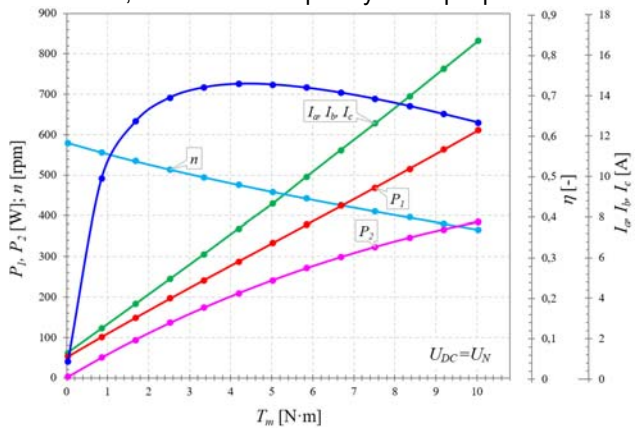

Fig.14. Electromechanical characteristics of the motor

Using the computed waveforms, the electromechanical characteristics of the motor were determined. They are shown in Figure 14. These characteristics are similar to those of a classic, separately excited, commutator motor. The mechanical characteristic is linear, as is the effective phase currents (I_a, I_b, I_c) – torque (T_m) relationship. The results of the computation confirmed the assumed motor parameters.

Conclusions

An external rotor BLDC motor was designed for a hoverboard. A field-circuit model of this machine was developed. It was used to carry out an analysis of the influence of the angle of permanent magnets and the shape of the stator slots on the values of the cogging and electromagnetic torques. On the basis of electromagnetic computations, the final motor design was selected. Analysis of the influence of the load torque on the motor's electrical and mechanical quantities waveforms was carried out, due to which the electromechanical characteristics were determined. The developed field-circuit model can be used to further analyse the operation of a brushless DC motor intended to drive a hoverboard.

Authors: *MSc Kinga Tokarska, E-mail: kinga_tokarska@outlook.com; Prof. Pwr, dr hab. Marek Ciurys, Electrical Engineering Faculty at Wroclaw University of Science and Technology, Wybrzeze Stanislawa Wyspianskiego 27, 50-370 Wroclaw, E-mail: marek.ciurys@pwr.edu.pl*

LITERATURE

[1] Aldosry, A.M., Zulkifli, R., Wan Ghopa, W.A., Heat Transfer Enhancement of Liquid Cooled Copper Plate with Oblique Fins for Electric Vehicles Battery Thermal Management, *World Electric Vehicle Journal,* 12 (2021), 55

[2] Mazan B., Detka T., Eksperymentalne badanie wpływu temperatury ogniwa litowojonowego na pojemność i dokładność obliczeń stopnia naładowania, *Maszyny Elektryczne - Zeszyty Problemowe*, (2019), nr 2, 185-190

[3] Fujita H., Itoh A., Urano T., Newly Developed Motor Cooling Method, *World Electric Vehicle Journal*, 10 (2019), 38

[4] Będkowski B., Madej J., Wyznaczenie zalecanego minimalnego natężenia przepływu czynnika chłodzącego dla układu chłodzenia silnika elektrycznego do zabudowy w kole, *Maszyny Elektryczne - Zeszyty Problemowe*, (2019), nr 2, 63-69

[5] Chong Y. C., Staton D., Gai Y., Adam H., Popescu M., Review of advanced cooling systems of modern electric machines for EMobility application, *2021 IEEE Workshop on Electrical Machines Design, Control and Diagnosis (WEMDCD)*, Modena, Italy, 2021

[6] Wiśniewski J., Kania A. i Witkowski Ł., Kompedium elektromobilności, Warszawa: Polskie Stowarzyszenie Paliw Alternatywnych, (2020), 149-154

[7] Dukalski P., Wolnik T., Będkowski B., Jarek T., Analiza pracy silnika zabudowanego w piaście koła samochodu osobowego dla wybranych parametrów jazdy, *Maszyny Elektryczne - Zeszyty Problemowe*, (2018), nr 1, 69-74

[8] Portal Gov.pl, „Polska przystępuje do Electric Vehicles Initiative (EVI)", 2020. [Online]. Available: https://www.gov.pl/web/klimat/polska-przystepuje-do-electric-vehiclesinitiative-evi. [Dostęp: 26.05.2021]

[9] International Energy Agency, „Global EV Outlook 2021", 2021. [Online], https://www.iea.org/reports/global-ev-outlook-2021/introduction#abstract. [Dostęp: 26.05.2021]

[10] Research and Markets, „Global Hoverboard Market to Reach US$1.9 Billion by the Year 2027" 2020. [Online], https://www.globenewswire.com/newsrelease/2020/12/31/2152016/28124/en/Global-Hoverboard-Market-to-Reach-US-1-9-Billion-by-the-Year-2027.html. [Dostęp: 17.01.2024]

[11] Carrasco Vergara P., Garcia Romero M. D. C. y., Macias Vecino M. A., Sistema de propulsión de carros y sillas de ruedas mediante patinete eléctrico de tipo hoverboard. Spain Patent 2 737 728, 15 01 2020

[12] Tokarska K., Ciurys M., Silnik BLDC do napędu pojazdu elektrycznego, *Stowarzyszenie Elektryków Polskich na Politechnice Wrocławskiej, Trendy i rozwiązania technologiczne w elektrotechnice*, Oficyna Wydawnicza Politechniki Wrocławskiej, ISBN 978-83-7493-190-8, Wrocław, 2021, 93-103

[13] Tokarska K., Silnik BLDC do napędu pojazdu elektrycznego, Magisterska praca dyplomowa, Wydział Elektryczny Politechniki Wrocławskiej, 2021